A microcalorimeter for measuring heat effects of electrochemical reactions with submonolayer conversions

ARTICLE *in* THE REVIEW OF SCIENTIFIC INSTRUMENTS · MARCH 2010

Impact Factor: 1.61 · DOI: 10.1063/1.3309785 · Source: PubMed

3 AUTHORS, INCLUDING:

Katrin R. Bickel
Technische Universität München
8 PUBLICATIONS **41** CITATIONS

SEE PROFILE

A microcalorimeter for measuring heat effects of electrochemical reactions with submonolayer conversions

Kai D. Etzel, Katrin R. Bickel, and Rolf Schuster[a)]
Institut für Physikalische Chemie, Karlsruhe Institute of Technology, D-76131 Karlsruhe, Germany

(Received 16 November 2009; accepted 16 January 2010; published online 3 March 2010)

We present a microcalorimeter for measuring heat effects during electrochemical reactions with conversions down to a few percent of a monolayer, referenced to the electrode's surface atoms. The design uses a thin pyroelectric polymer foil for temperature measurement at the backside of a thin electrode, similar to the concepts pioneered by the groups of D. A. King and Ch. T. Campbell for UHV adsorption microcalorimetry. To establish intimate thermal contact between electrode and sensor and utmost sensitivity, the free standing sensor and electrode foils are pressed together by air pressure, acting on the electrochemical cell. Pyroelectric temperature sensing is combined with pulsed electrochemistry, where the electrochemical heat is released on a time scale of about 10 ms, which is long enough for thermal equalization of the electrode-sensor assembly but short enough to avoid significant heat loss into electrolyte and cell compartment. As examples heat effects upon Ag deposition and dissolution as well as the electron transfer reaction of $[Fe(CN)_6]^{4-}/[Fe(CN)_6]^{3-}$ are presented. The latter reaction was also employed for the calibration of the calorimeter.
 [doi:10.1063/1.3309785]

I. INTRODUCTION

Measuring heat effects of electrochemical reactions dates back to the 19th century, when Bouty studied electrochemical copper dissolution and deposition.[1] He employed copper covered thermometers as electrodes and was able to detect tiny temperature variations upon strong macroscopic bulk deposition or dissolution of Cu, respectively. In analogy to the heat effects accompanying current flow through metal junctions, he named the effect after Peltier. Indeed, as investigated by Lange and co-workers in the 1930s[2,3] and precisely formulated by Agar in 1963,[4] for electrochemical reactions conducted close to the thermodynamic equilibrium, the heat effects reflect the overall entropy change at the metal-electrolyte interface. Peltier coefficients, i.e., molar heats of electrochemical (half-cell) reactions, were determined for various, apparently "simple," electrochemical reactions such as Ag and Cu deposition or Fe(II)/Fe(III) electron transfer reactions. For reactions with a well defined potential of electrochemical equilibrium (i.e., Nernst potential) the measured Peltier heats are directly related to the entropy of reaction for the respective system and can therefore be directly compared with entropy values derived from the temperature dependence of the equilibrium potential. More complicated processes, where the electrochemical reactions may be accompanied by partly irreversible chemical reactions, were only scarcely studied. Examples are electrochemical water formation from the elements,[5] hydrogen and oxygen evolution,[6,7] charging and discharging of batteries,[8,9] and corrosion processes.[10] In those examples the evolved heat is only partly caused by the entropy of the electrochemical reaction and the measured heat may provide information on the reaction pathway and irreversible processes. However, all the cited experiments required macroscopic conversions of tens to hundreds of atoms per electrode's surface atom, in order to obtain detectable heat effects. On the other hand, calorimetric studies of the first steps of electrochemical reactions, e.g., the deposition of the first metal layer or the hydrogen adsorption, which precede bulk metal deposition or hydrogen evolution, respectively, may be desirable to shed light on elementary steps of electrochemical reactions.

In principle, there exist two experimental approaches for measuring heat evolution upon electrochemical reactions. In the first approach, pioneered by Lange and co-workers in the 1930s,[2,11,12] the complete half-cell consisting of electrode and electrolyte is kept in thermal equilibrium and the evolved heat is measured in an adiabatic or isothermal calorimeter. Due to the large heat capacity of the whole cell compartment, the sensitivity of those measurements is rather poor, requiring high electrochemical conversions. On the other hand, absolute values for the Peltier heats can be readily obtained with high precision.[13,14] In the second approach the transient temperature difference between electrode and electrolyte is measured, e.g., via a thermocouple or a thermistor. The Peltier heat is determined either from the rate of the temperature change briefly after the initiation of an electrochemical reaction or from the steady temperature difference, which is reached when the heat flow into electrolyte and surrounding is balanced by the rate of the heat evolution. This approach was applied by Bouty in his early experiments[1] and later improved, e.g., by Bružs, Ozeki, or Kuz'minskii.[6,7,15–17] Quantitative measurements of heat effects require either careful calibration or detailed knowledge of the heat flow and thermal properties of the cell. However,

[a)]Author to whom correspondence should be addressed. Electronic mail: rolf.schuster@kit.edu. Telephone: +49 721 608 2102.

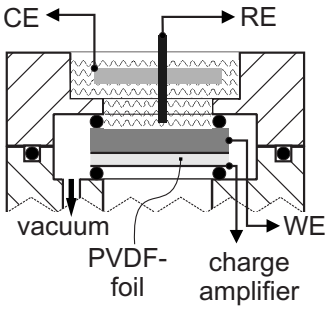

FIG. 1. Schematic of the cell. The thin WE is mounted directly onto the free-standing pyroelectric detector foil. Thermal contact is established by removing the air in between electrode and detector foil (RE: reference electrode and CE: counter electrode).

due to smaller heat loss into the electrolyte the latter approach is inherently more sensitive compared with the first one, employing a calorimeter, where the whole (half-) cell compartment is at thermal equilibrium.

Although most of the older work required high electrochemical conversions, the detection of heat effects originating from a surface process, namely, the adsorption of hydrogen on Pt was successfully demonstrated by Shibata *et al.*[18] In order to obtain detectable changes in temperature, a platinized Pt electrode with high surface area was used. Recently the optical detection of temperature variations by deflection of a light beam, due to the change in the refractive index with temperature was demonstrated by Hai and Scherson[19] for the oxidation and reduction in a monolayer (ML) of a Au surface in hydrosulfuric acid.

Here we present a novel experimental realization of an electrochemical microcalorimeter, which allows to detect heat effects originating, e.g., from the formation of a few percent of a Cu underpotential-deposited layer on a smooth Au surface or the $[Fe(CN)_6]^{4-}/[Fe(CN)_6]^{3-}$ redox reaction with similar conversions. To obtain such sensitivity, in our approach: (i) a freely suspended polyvinylidene fluoride (PVDF) foil is used as temperature sensor at the back side of a thin (about 10–100 μm) electrode and (ii) the electrochemical experiments are conducted with short potential or current pulses of the order of 10 ms. This pulse duration is long enough to establish thermal equilibrium across the electrode-sensor assembly and short on the time scale of heat losses into the electrolyte and the surrounding electrode mount. Intimate thermal contact between sensor foil and electrode is established by removing the air in between the sensor and the electrode, whereby both are pressed together by the air pressure, acting on both sides of the electrode-sensor assembly. Preliminary data were already presented in Ref. 20. Here we will, in detail, describe an improved experimental setup and discuss strategies for the calibration of the calorimeter and possible sources of error.

Measuring temperature changes of thin, freely suspended samples was introduced by King's group for the measurement of heats of adsorption of gases on single crystal surfaces under UHV conditions.[21] While first experiments employed infrared temperature sensing, the sensitivity was significantly increased by the use of a PVDF foil as temperature sensor by Campbell's group.[22,23] It should be noted that PVDF foils were used as temperature sensors for microcalorimetry before, e.g., for the detection of thermal effects upon nerve action[24] or even in electrochemical experiments.[25] However, none of these approaches used a freely suspended electrode sample assembly which resulted in a high effective heat capacity of the sensor and reduced sensitivity.

II. EXPERIMENT

A. Cell design

The calorimeter is schematically shown in Fig. 1. The pyroelectrically sensitive PVDF foil (typically 9 μm thick) is mounted directly at the backside of the electrode. For the current experiments the working electrode (WE) consisted of 50 μm thick Au foils which were freely suspended. Alternatively, thin Au films evaporated onto 120 μm Si-sheets or 12.5 μm thick Au foils supported by 120 μm Si-sheets were employed as electrodes. In order to achieve intimate contact between the sensor and the electrode, the electrode-sensor assembly was sealed on both sides with O-rings and air was removed from the gap in between sensor and electrode. The outside air pressure, acting on both sides of the electrode sensor assembly, presses both foils together and ensures good and reproducible thermal contact. In the case of an additional 120 μm Si support the Si-sheet is tightly clamped in between the sensor foil and the electrode foil by the outside air pressure and no degradation of the thermal contact by the additional sheet was discernible in the present experiments. In fact, the electrochemical experiments in Secs. IV and V were all conducted with a Si support and a 12.5 μm Au foil in order to avoid mechanical deformation of the sensor assembly by electrostriction.[20]

The upper part of the calorimeter was manufactured from KEL-F® and served as electrolyte compartment for the electrochemical cell. KEL-F® possesses similar chemical inertness as Teflon but better mechanical strength. The active electrode area had a diameter of 5 mm. A Pt-ring or alternatively a flat spiral, wound from ∅0.5 mm Pt-wire served as counter electrode (CE). The reference electrode (RE) consisted of a ca. ∅0.5 mm wire which was insulated by a Teflon tube up to the very end of the electrode and which was mounted in close proximity to the WE in order to minimize the ohmic potential drop between RE and WE. Dependent on the experiment Ag-, Pt-, or hydrogen loaded Pd-wires were used as REs. The whole cell compartment was enclosed in an air tight container (not shown) and could be operated under inert atmosphere. The container had thick brass walls and was enclosed by thermally insulating foam.

To collect the charge of the pyroelectric sensor, both sides of the PVDF foil were coated with Al. While the front side was completely covered with Al, on the rear side of the sensor a ∅4 mm circular Al pad served as electrode. Therefore, only the temperature of the inner part of the electrode was measured which minimized the capacitance of the sensor and reduced the influence of heat losses into the electrode holder during the temperature transients.

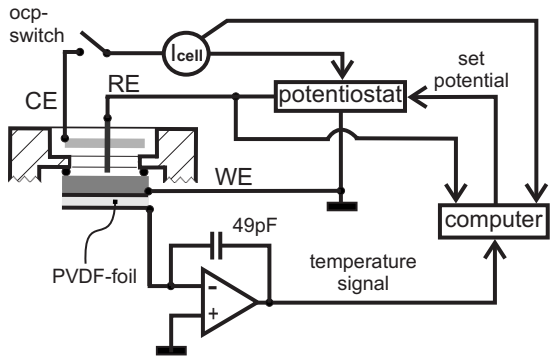

FIG. 2. Sketch of the electronic circuit. The pyrolectric signal is collected at the backside of the metallized PVDF foil, referenced to the WE. The electrochemical cell current (I_{cell}) is measured at the CE. The cell can be electrically switched off by the computer controlled ocp-switch (RE: reference electrode and CE: counter electrode).

B. Experimental setup

In Fig. 2 the setup of the experiment is sketched. The electric potential of the WE was controlled by a homebuilt potentiostat. Since the WE was directly touching the Al-coated PVDF sensor foil, it was grounded in order to provide a stable reference for the measurement of the pyroelectrically generated charge. The electrochemical current was measured in the current path to the CE. In order to completely cut off the external current flow to the CE and to stop electrochemical reactions on demand, the electrochemical cell could be switched to "open cell" conditions by a computer controlled switch (ocp-switch). The set potential of the potentiostat was completely computer controlled and could be varied with a time response of about 10 μs. It should be noted that the potentiostat could be switched to galvanostatic operation at any time during the experiment. The set current was also controlled by the computer with about 10 μs time resolution. For clarity the galvanostatic option is omitted in Fig. 2.

The charge at the sensor foil accumulated during the temperature transient was measured by a charge amplifier at the rear side of the sensor, referenced to the grounded front side. The output of the charge amplifier directly corresponds to the temperature change of the sensor foil. As an alternative route, one could directly measure the current produced by charge accumulation at the foil during the temperature transient with a conventional current voltage converter, followed by integration in order to obtain the temperature signal. However, in a typical experiment the pyroelectric currents are of the order of picoamperes, which have to be measured with a time resolution better than 1 ms in order to follow the electrochemical transients. Conventional current to voltage converters suffer from limited time resolution at high sensitivity, i.e., high conversion factors, due to stray capacitances in the feedback loop and the operational amplifier input. Hence, fast current transients may be significantly distorted by the current to voltage converter, which may cause significant errors for the measured temperature. We therefore decided for directly integrating the pyroelectrically generated current in the feedback capacitance of the charge amplifier, which is advantageous for accurately measuring fast temperature transients. The temperature transient, potential of the RE, and electrochemical cell current were simultaneously recorded by the computer during the experiment.

C. Typical experimental procedure

Au electrodes were cut from polycrystalline Au foils (99.999%; Wieland) of 50 μm thickness, cleaned in hot H_2O_2/H_2SO_4 and flame annealed in a butane or hydrogen flame. Alternatively, 12.5 μm thick Au foils (99.99%; Advent) were prepared as described above and placed onto a Si-sheet [n-Si(111), 120 μm thick, supplied by Siltronix], which was then mounted on the sensor foil. Although the 12.5 μm Au foils could be directly placed onto the sensor foil, the stiff intermediate Si-sheet effectively suppresses distortions of the temperature signal due to electrostriction, i.e., changes in the electrode's surface tension during electrochemical polarization and consequent mechanical deformations.[20]

$AgClO_4$ solutions were prepared by dissolution of Ag_2O (suprapure, Merck) in $HClO_4$ (suprapure, Merck). For the preparation of the $K_4[Fe(CN)_6]/K_3[Fe(CN)_6]$ solution analytical grade chemicals were used (Merck). Ultrapure water was supplied by an Arium system (Sartorius). The electrolytes were usually purged with nitrogen, however, for the experiments presented here, no influence of dissolved oxygen on the observed results was found. Before assembling the cell, all parts of the cell were immersed in hot H_2O_2/H_2SO_4 solution and thoroughly rinsed with ultrapure water. Cyclic voltammograms were recorded directly in the cell prior to the temperature measurements.

After assembling and filling the cell, the thermal equilibration of the system took about 10 min before calorimetric measurements commenced. The values of the temperature change during the electrochemical reaction are referenced to the electrode temperature immediately before the application of the potential pulse. Heat values are referenced to the electrode-sensor assembly in accordance with the definition of the Peltier heat for electrochemical reactions, i.e., positive heat values correspond to warming of the electrode or heat transfer from the electrochemical interface to the electrode. Electrochemical conversion is usually presented as charge density. For comparison the values of the electrochemical conversion are also given in units of ML, where 1 ML refers to one reacted ion or atom per surface atom of a perfectly flat, densely packed (111) electrode. Roughness or crystalline orientation of the surface are not considered.

III. THERMAL RESPONSE OF THE ELECTRODE-SENSOR ASSEMBLY

One of the key aspects of our experiment is the thermal response of the electrode-sensor assembly. It should quickly equilibrate in order to measure the temperature change at the electrode surface during the electrochemical reaction without delay. On the other hand, the temperature measurement should not be influenced by heat flow to the electrolyte or cell holder or by uptake of Joule heat stemming from electric current flow through the electrolyte. In order to test the thermal response, we irradiated the electrode surface, *in situ*, i.e.,

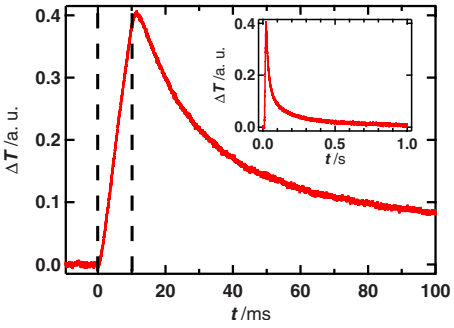

FIG. 3. (Color online) Temperature response of the electrode-sensor assembly to a 10 ms laser pulse of ≈5 mW. Pulse start and end are indicated by dashed lines. The inset shows the temperature transient up to $t=1$ s.

immersed in electrolyte or water with a diode laser. The laser was strongly defocused and only part of the beam profile hit the electrode surface to ensure rather homogeneous warming of the electrode. The power of the laser beam was monitored via a beamsplitter by a photodiode. Figure 3 shows the temperature response of a 50 μm thick Au foil upon irradiation with a 10 ms laser pulse with constant laser output power of around 5 mW. The sensor temperature started to rise almost immediately after the beginning of the pulse (at $t=0$) with a delay of only a few 100 μs. The constant laser irradiation during the pulse is reflected by an approximately linear temperature increase. After switching off the laser irradiation, the temperature signal slightly overshot, reaching its maximum about 2 ms after the end of the pulse. Afterwards the temperature decreased over several 100 ms (inset in Fig. 3), signaling temperature equalization with the electrolyte and the surrounding. It should be noted at this point that the electronic discharging time constant of the charge amplifier amounts to about 5 s, which is by far longer than the observed transients and should therefore not distort the temperature measurement in our experiments. Initially, the decay of the temperature occurred rather fast with a half-value period of about 25 ms, whereas it took of the order of 0.3 s to reach the initial value within 10%. Laser irradiation without electrolyte led to an only slightly retarded temperature decay, which indicates that a significant part of the heat generated by the laser pulse, was transferred to the electrode mount.

Regarding the small thickness and the good thermal conductivity of the Au electrode, the fast response of the sensor to the laser pulse with a delay of only a few 100 μs seems conceivable. In order to estimate the typical timescale for temperature variations across the thickness of the electrode, we considered the time for temperature equalization across an infinite plate with thickness d, whose front side is brought to a different temperature at $t=0$. According to Ref. 26 the temperature profile across the thickness of the plate equalizes to about 10% within a time $\tau=d^2\alpha^{-1}$, where the thermal diffusivity α is given by $\alpha=\lambda/(\rho c)$. λ is the thermal conductivity, ρ the density, and c the specific heat of the material. For polycrystalline Au $\lambda=3.17$ W cm^{-1} K^{-1}, $\rho=19.3$ g cm^{-3}, and $c=0.129$ J g^{-1} K^{-1},[27] which for a 50 μm foil results in $\tau\approx 20$ μs. We have no estimate for the thermal resistance across the Au-PVDF contact, however, because of the intimate contact between both foils, the small thickness of the pyroelectric foil (9 μm) and its low heat capacitance, we expect that the sensor would almost instantaneously follow the Au temperature. In conclusion, we expect that for the temperature transients measured on a time scale of 10 ms, only minute temperature differences occur between the front and the backside of the electrode, in comparison with the total temperature change.

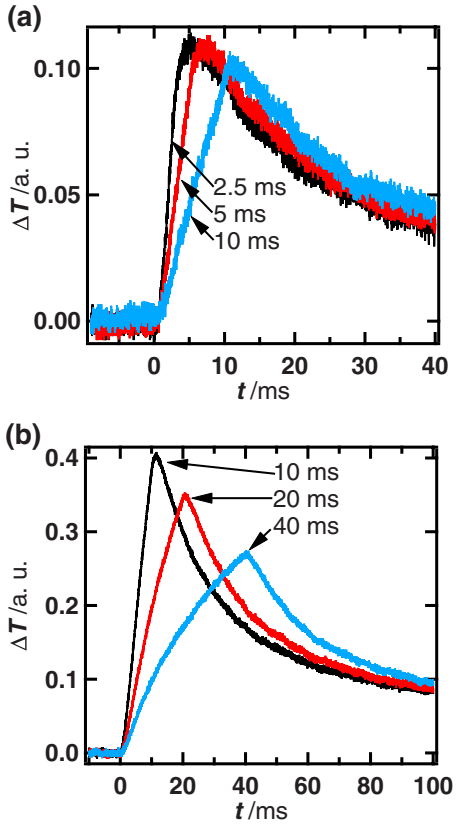

FIG. 4. (Color online) Temperature response to laser pulses with varying pulse duration but identical total energy. (a) 2.5, 5, and 10 ms pulses, around 12.5 μJ per pulse. (b) 10, 20, and 40 ms, around 50 μJ per pulse.

The linear increase in the temperature signal during the constant power laser pulse already demonstrates that the temperature signal is to a good approximation proportional to the heat uptake during the pulse. A steady state, where heat uptake is balanced by heat flow to the surrounding, is far from being reached within the 10 ms pulse duration. However, the rather fast decay of the temperature after the pulse implies that heat losses to the surrounding will lower the measured temperature already during the pulse. Therefore, the temperature at the end of the pulse should slightly depend on temporal variations in the laser power during the pulse even if the total absorbed heat is kept constant. In order to estimate the variations in the temperature at the end of the pulse under extreme power variations during the laser pulse, we performed experiments where the duration of the laser pulse was varied. The total energy of the laser pulse, as monitored by integrating the photodiode signal, was kept constant by adjusting the pulse power. In Fig. 4(a) temperature transients of 2.5, 5, and 10 ms laser pulses with identical total heat uptake are shown. Measuring the change in temperature 10 ms after the beginning of the pulses leads to about the same temperature for all three transients (within 5%), signal-

ing that the sensor temperature at 10 ms is a good measure for the total absorbed heat, irrespective of the distribution of the laser power during the pulse period. It should be noted that the good agreement among the different laser pulses is partly caused by the temperature overshoot after the end of the pulses. The temperature overshoot is considerably larger for shorter pulse durations. However, the time delay between the end of the pulse and the temperature maximum is approximately constant and amounts to about 2 ms. Therefore, for the shorter laser pulses the temperature at 10 ms includes the temperature overshoot, whereas for 10 ms pulses the temperature overshoot follows afterwards which partly compensates for heat losses during the pulse. Indeed, after crossing the temperature maximum the transient of the 10 ms laser pulse lies considerably (around 15%) above those of the shorter pulses.

In order to explore the origin of the temperature overshoot, we conducted experiments with a 120 μm thick Si-sheet, coated with 200 nm Au as electrode. With the Si-sheet the temperature overshoot was delayed by 5 ms (data not shown), which is more than twice the delay observed with the Au electrode. Hence, the temperature overshoot has to be attributed to the thermal properties of the electrode material. Indeed, the thermal diffusivity of Si is about 1/2 of that of Au, which should be directly reflected in a longer timescale for temperature variations and equalization after the pulse. Whereas equalization of the temperature across the thickness of the sensor-electrode assembly should occur on timescales less than 100 μs (see discussion above), lateral temperature variations due to heat conduction to the edge of the electrode foil and into the sample holder will build up or equalize on a much longer timescale. The typical length for lateral temperature variations is in the order of millimeters in our experiment, which is more than 20 times larger than the thickness of the Au electrode. Applying the above approximation for the one-dimensional temperature equalization across an infinite plate, we expect typical time scales for lateral temperature variations in the order of milliseconds which is in good agreement with the observed delay of the temperature maximum. Exchanging Au for Si is expected to double the delay, as experimentally observed. We therefore attribute the temperature overshoot to variations in the lateral temperature profile due to heat conduction into the edge of sample and sample holder before a steady temperature profile is established.

In Fig. 4(b) temperature transients for laser pulses with up to 40 ms duration are shown. Analogously to the transients in Fig. 4(a) the total absorbed heat during the laser pulses was kept constant. Its value was increased by a factor of four in comparison with the pulses of Fig. 4(a), which is reflected in the improved signal-to-noise ratio of the recorded temperature signal. Application of 20 or 40 ms pulses resulted in nonlinear temperature rises, signaling considerable heat transfer to the surrounding already on that time scale. Indeed, after prolonged laser irradiation of more than 1 s, the temperature change "saturated," indicating that a steady state was reached, where heat uptake from the laser was balanced by heat loss to the surrounding (data not shown). However, at pulse durations of 40 ms, less than 10%

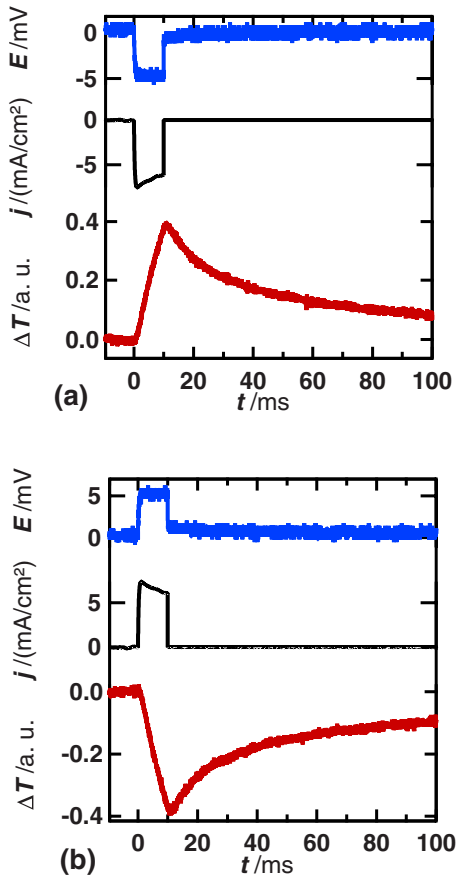

FIG. 5. (Color online) Potential (E), temperature (ΔT), and electrochemical current (j) transients upon pulsed Ag dissolution (a) and deposition (b) onto around 300 ML thick Ag layer on Au. (20 mM $AgClO_4$/1 M $HClO_4$, 12.5 μm Au foil, supported by 120 μm thick Si). Before the potential pulse, the cell potential was set to the Ag/Ag^+ equilibrium potential (E=0). At t=0 the potential was stepped 5 mV positive (a) or negative (b). After 10 ms the cell current was forced to 0 by opening the ocp-switch.

of the steady state temperature change was reached. The temperature measured 40 ms after the beginning of the three pulses in Fig. 4(b) varied by 40% (referenced to the 40 ms pulse) depending on the temporal distribution of the laser power. Hence, it can be concluded that for our experimental setup the heat released by electrochemical reactions should be measured within about 10 ms after the beginning of the reaction. On this time scale the measured temperature well reflects the evolved heat, irrespective of temporal variations in the rate of heat evolution, i.e., variations in the faradaic current. In principle, also for longer time scales the evolved heat could be reconstructed from the electrode temperature, however, this would require precise knowledge of the thermal properties of the electrode and the cell and probably elaborated simulations of the sensor temperature.

IV. TEMPERATURE TRANSIENTS UPON PULSED SILVER DEPOSITION AND DISSOLUTION

Temperature transients of pulsed deposition and dissolution of Ag from a 20 mM $AgClO_4$/1 M $HClO_4$ solution are depicted in Fig. 5, together with the respective potential and cell current transients. Before recording the transients, about 300 ML of Ag were electrochemically deposited onto a 12.5 μm thick Au foil supported by a 120 μm Si-sheet.

Afterwards the cell potential was adjusted for zero cell current, i.e., to the Nernst potential for Ag/Ag^+ in the respective solution.

In Fig. 5(a) a negative potential pulse of 5 mV was applied for 10 ms, leading to instantaneous deposition of Ag with current densities up to about 7.5 mA/cm^2. The total deposited amount of Ag during the pulse, as calculated from the electrochemical charge, amounts to around 30% of a monolayer of Ag, referenced to the number of Ag atoms in a densely packed Ag(111) surface. During the metal deposition the electrode temperature increased with time, signaling heat uptake from the electrochemical reaction. The approximately linear slope of the temperature graph is directly conceivable from the approximately constant faradaic current which decreases by only 20% during the short deposition pulse. The sign of the heat effect, i.e., the evolution of heat during silver deposition is well understood from experiments of Lange and co-workers[2,4] and can be directly attributed to the reduction of the entropy of the electrode-solution interface by the transition of Ag ions from solution to binding sites at the electrode. It should be noted that the overpotential to drive the reaction is fairly low, due to the high exchange current density of the Ag/Ag^+ reaction. Therefore, the Ag deposition or dissolution reactions in our experiments are conducted close to equilibrium conditions and the heat evolution can be discussed almost entirely in terms of entropy changes. Heat evolution, due to deviations from thermal equilibrium, i.e., irreversible heat, which would always lead to warming of the electrode, will contribute only a small fraction of the measured heat. This will be considered in more detail upon discussing Fig. 7 below. Furthermore, capacitive charge, stemming from charging of the electrochemical double layer upon polarization, is rather negligible if compared with the large faradaic charge. In fact, assuming a double layer capacitance of 50 $\mu F/cm^2$ and a polarization by 5 mV, the capacitive charge amounts to only 0.25 $\mu C/cm^2$ which corresponds to about 0.5% of the total charge. After the potential pulse the electrochemical reactions were stopped by switching off the cell current via the ocp-switch. The potential steps back close to the initial potential and the temperature starts to decay almost immediately, with a very short delay of 2 ms, similarly to the laser pulse experiments described above.

The heat effects upon Ag dissolution are depicted in Fig. 5(b). Upon Ag dissolution the entropy of the electrode-solution interface increases due to the production of Ag^+ ions. Thus, the temperature of the electrode decreases. Again, the faradaic current is only slightly varying during the dissolution, which is reflected by an about linear reduction in the temperature with time, i.e., an about constant rate of heat uptake during the electrochemical reaction. After the cell is set to ocp the potential relaxes to the equilibrium potential corresponding to the current state of the surface. The amount of dissolved Ag in this experiment corresponds to about 30% of a monolayer.

By increasing the overpotential, i.e., the amplitude of the potential pulse which drives the Ag deposition or dissolution reactions, faradaic current densities up to 50 mA/cm^2 (measured at the end of the potential pulse) were achieved. Due to short pulse duration and considerably high Ag-concentration

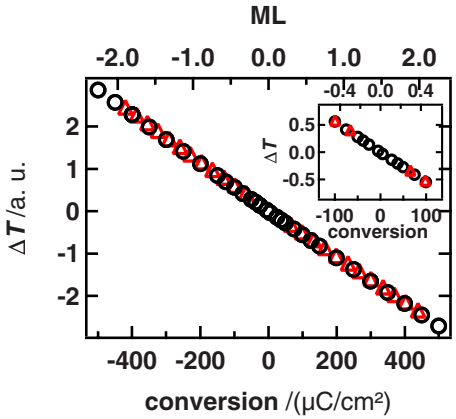

FIG. 6. (Color online) Temperature change, measured 10 ms after the beginning of the potential pulse for different electrochemical conversion, i.e., electrochemical charge density upon deposition or dissolution of Ag in 20 mM $AgClO_4$/1 M $HClO_4$. Prior to the experiments, around 300 ML Ag were deposited onto the Au electrode. For comparison the electrochemical conversion is also given in ML of Ag, assuming one transferred elementary charge per Ag atom in a Ag(111) surface. Triangles: data measured potentiostatically with constant amplitude potential pulses. Circles: data measured galvanostatically, i.e., with constant current during the deposition or dissolution pulse. The inset shows a closeup for low conversions.

in the electrolyte solution, the diffusion limit was not reached during the pulses. In Fig. 6 the change in the electrode temperature measured 10 ms after the beginning of the potential pulse is plotted versus electrochemical conversion, given as charge, which flowed during the pulse. As discussed above, this temperature is expected to correspond to a good approximation to the heat evolved during the reaction. Two data sets, measured potentiostatically with constant potential during the pulses and galvanostatically with constant current during the pulse, are included in the figure. For comparison we also calculated the amount of Ag which was deposited or dissolved during the reaction by assuming one elementary charge per Ag atom, thereby ignoring charging of the double layer as well as possible accompanying anion desorption or adsorption. The measured change in temperature varies linearly with the charge, i.e., the deposited or dissolved amount of Ag. Both processes, dissolution and deposition, exhibit the same slope of the heat versus charge, signaling almost perfect reversibility of the studied reaction under the applied conditions, i.e., on a time scale of 10 ms with current densities up to 50 mA/cm^2.

V. CALIBRATION OF THE SENSOR

Since heat losses of the sensor-electrode assembly to the electrolyte and the cell compartment depend on many experimental parameters, which are not precisely known, the sensor has to be calibrated. In principle the thermal response upon well defined heat uptake, e.g., from a laser pulse could be used for calibration. This approach was applied for example by Borroni-Bird and King[21] for calibration of their UHV calorimeter and requires careful determination of the reflectivity of the sample surface and consideration of stray light from usually slightly rough surfaces. For calibration of our microcalorimeter we chose direct comparison of our heat signal with Peltier coefficients known for bulk electrochemi-

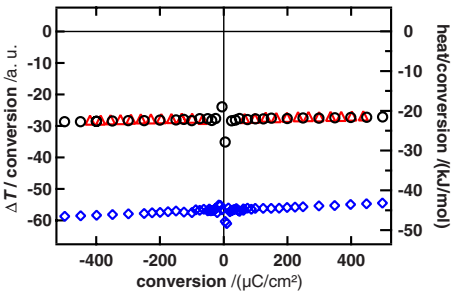

FIG. 7. (Color online) Temperature change normalized to the electrochemical conversion, measured with 10 ms potential pulses for the Fe(II)/Fe(III) electron transfer reaction in 0.1 M $K_4[Fe(CN)_6]$/0.1 M $K_3[Fe(CN)_6]$ (diamonds) and the Ag/Ag^+ ion transfer reaction in 20 mM $AgClO_4$/1 M $HClO_4$ (triangles: potentiostatic pulses; circles: galvanostatic pulses). The right axis was obtained by calibration of the calorimeter with the help of literature data (see text).

cal reactions. Care has to be taken in choosing the respective electrochemical reaction, since our data are measured with submonolayer electrochemical conversions where parallel surface processes such as anion adsorption may strongly contribute to the heat effects. In contrary, the Peltier coefficients known from literature were usually measured with conversions of hundreds of monolayers, where minute changes of the electrode surface were irrelevant. Considering these aspects, we chose the electron transfer reaction in the $[Fe(CN)_6]^{4-}/[Fe(CN)_6]^{3-}$ redox system as reference. Electron transfer reactions should not involve modifications or side reactions on the electrode surfaces, besides charging of the double layer. Furthermore, the $[Fe(CN)_6]^{4-}/[Fe(CN)_6]^{3-}$ redox reaction exhibits a relatively high Peltier coefficient which was carefully measured by several groups (e.g., Refs. 28 and 29). In addition, the reaction can be driven with high current densities at relatively low overpotentials which is important to minimize the amount of irreversible heat.

In Fig. 7 the temperature changes normalized to the electrochemical conversion, i.e., the flowed charge, are depicted in arbitrary units versus conversion for 0.1 M $K_4[Fe(CN)_6]$/0.1 M $K_3[Fe(CN)_6]$. Analogous to the Ag experiments discussed above, the temperature of the electrode was measured after a 10 ms potential pulse. The charge, which flowed during the 10 ms, was controlled either by applying rectangular potential steps with different amplitudes or by galvanostatically controlling the cell currents. The experiments were conducted on a 12.5 μm Au foil which was supported by a 120 μm thick Si-sheet. In Fig. 7 we also included data for Ag deposition and dissolution from 20 mM $AgClO_4$ on Ag which were derived from the measurements depicted in Fig. 6. Negative values of the normalized temperature change correspond to cooling of the electrode upon oxidation or warming upon reduction, respectively, in accordance with the sign of the temperature transients in Fig. 5. Note the slight variation of the normalized change in temperature with conversion. Obviously, the electrode becomes less cold than expected from a linear relationship between heat evolution and electrochemical conversion, when the oxidation is conducted with larger (positive) current densities and vice versa, upon reduction with larger (negative) currents the electrode stays warmer than expected. In other words, we observe surplus heat evolution at high conversions which we attribute to irreversible heat evolved at high overpotentials. As discussed above, the double layer capacitance is neglected in the conversion or charge values since its contribution to the total charge is rather small. Furthermore, correcting for capacitive charge would lower the absolute value of the charge and would hence shift the values of the normalized temperature change in Fig. 7 in the same direction for both oxidation and reduction. Therefore, capacitive charge cannot account for the observed variations in the normalized temperature change with electrochemical conversion.

In order to extract Peltier heat from Fig. 7, which are by definition derived for reversible reactions, we extrapolated the measured normalized temperature change toward zero conversion, which yielded a value of 56.7×10^3 a.u. corresponding to the Peltier heat of a 0.1 M $K_4[Fe(CN)_6]$/0.1 M $K_3[Fe(CN)_6]$ solution. Wang *et al.*[29] gave a value of -41.48 ± 2.39 kJ/mol for the Peltier heat in the same solution, Boudeville *et al.*[28] measured -45.35 ± 1.785 kJ/mol. Accepting Boudeville's value for calibration of our calorimeter, our measurements yield a Peltier heat of Ag/Ag^+ in 20 mM $AgClO_4$/1 M $HClO_4$ of -24 kJ/mol, as derived from the Ag data in Fig. 7. This should be compared to the measurements of Ozeki *et al.*,[16] who obtained a value of -28 kJ/mol in the same solution. The difference of about 20% between our measurements and the measurements of Ozeki may find its explanation in the different experimental procedures. Ozeki used electrochemical conversions of typically 20–200 ML. In contrast, our measurements with one to two orders of magnitude lower conversions may well include contributions from additional surface reactions which are not of relevance for bulk reactions. It should also be noted that the first steps of the deposition of Ag onto a surface involve the formation of a Ag adatom gas, whose nucleation and crystallization may not be finished within our 10 ms measurement period.[30,31] Although we expect that the ion transfer to the surface provides the largest contribution to the overall entropy loss during Ag deposition, the chemical state of the silver on the surface may well influence the entropy of the reaction. A Ag adatom gas is expected to exhibit higher entropy per atom than a well ordered Ag layer. Therefore, under our experimental conditions, i.e., within a 10 ms potential step, it is reasonable to expect a smaller entropy loss than upon slow Ag bulk deposition, which could account for the smaller Peltier coefficient found in our pulse experiments.

Within one series of experiments, i.e., without dismantling of the cell, the temperature transients were very reproducible. Under constant electrochemical conditions the values of the heat per conversion varied typically by less than 0.5 kJ/mol at intermediate conversions of about 0.5 ML. At lower conversions the noise of the temperature measurement increased and the reproducibility of the heat per conversion degraded. In our measurements we typically obtained a reproducibility of 2.5 kJ/mol for conversions as low as 0.05 ML within one series of experiments. After dismantling and reassembling the cell the Peltier coefficient of $[Fe(CN)_6]^{4-}/[Fe(CN)_6]^{3-}$ could be reproduced within about

8 kJ/mol without recalibration of the calorimeter. This signals the good reproducibility of the thermal contacts both across the electrode-sensor assembly and toward the cell mount. To eliminate this error the calibration of the sensor was typically checked at the end of every series of experiments by exchanging the electrolyte and measuring the Peltier coefficient of the $[Fe(CN)_6]^{4-}/[Fe(CN)_6]^{3-}$ electron transfer reaction.

VI. FUTURE IMPROVEMENTS

The study of surface electrochemical reactions often requires the use of well defined substrate surfaces. Up to now our experiments were conducted on polycrystalline substrates. In principle, thin single crystals could be used as electrodes, similar to those employed in UHV studies. Depending on their thickness, such crystals may be supported, for example, by Si-sheets, in order to avoid mechanical deformation due to electrostriction. A more simple approach is the use of thin metal films, deposited on solid substrates. As demonstrated above, around 120 μm thick Si wafers can be used as substrates without significant influence on the response time of the calorimeter. Au could be electrodeposited onto the Si surface in order to obtain well ordered and oriented Au surfaces.[32] For even better thermal response Si may be substituted by sapphire or diamond. For example, Au films prepared by Au evaporation onto sapphire can be flame annealed which results in a well ordered surface with large (111)-oriented terraces.[33]

The current sensitivity of the calorimeter allows the study of electrochemical reactions with conversion of the order of a few percent of a monolayer. Although this sensitivity is sufficient for investigations of most charge transfer reactions on electrodes, more subtle effects, such as ordering phenomena on surfaces or phase transitions where only minute changes of the entropy of the system are involved, will require higher sensitivity. In the current setup the sensitivity of the charge amplifier is not limited by electronic noise and could be readily increased by lowering the charge integrating capacitance at the expense of a slightly more unstable base line of the temperature signal and a shorter discharging time constant of the charge amplifier. We expect that the sensitivity of the charge amplifier could be enhanced by about one order of magnitude in this way. However, this may require additional means for temperature stabilization of the surrounding of the calorimeter and longer intervals in between the measurements in order to achieve equilibration of the cell.

In conclusion, our microcalorimeter allows for the detection of electrochemically generated heat down to conversions of a few percent of a monolayer for electron and ion transfer reactions. This includes underpotential deposition, e.g., of metals or hydrogen. The extension of the method toward study of phase transitions or adsorption phenomena, where only minute changes of the surface coverage are expected, seems to be within reach.

ACKNOWLEDGMENTS

We gratefully acknowledge technical support by E. Waltz and his colleagues during the construction of the calorimeter. Financial support was provided by Fonds der Chemischen Industrie.

[1] E. Bouty, Compt. Rend. **89**, 146 (1879).
[2] E. Lange and T. Hesse, Z. Elektrochem. **38**, 428 (1932).
[3] E. Lange and K. P. Miščenko, Z. Phys. Chem. Abt. A **149**, 1 (1930).
[4] J. N. Agar, in *Advances in Electrochemistry and Electrochemical Engineering*, edited by P. Delahay (Interscience, London, 1963), Vol. 3, p. 31.
[5] V. J. Cunnane, R. A. Scannell, and D. J. Schiffrin, J. Electroanal. Chem. **269**, 163 (1989).
[6] B. Bružs, Z. Phys. Chem. **145**, 470 (1929).
[7] Y. V. Kuz'minskii and A. V. Gorodyskii, J. Electroanal. Chem. **252**, 21 (1988).
[8] V. S. Donepudi and B. E. Conway, J. Electrochem. Soc. **131**, 1477 (1984).
[9] Y. Kobayashi, H. Miyashiro, K. Kumai, K. Takei, T. Iwahori, and I. Uchida, J. Electrochem. Soc. **149**, A978 (2002).
[10] A. T. Kuhn and A. M. S. e. Din, Surf. Technol. **20**, 55 (1983).
[11] E. Lange and T. Hesse, Z. Elektrochem. **39**, 374 (1933).
[12] E. Lange and J. Monheim, Z. Phys. Chem. Abt. A **150**, 177 (1930).
[13] J. M. Sherfey, J. Electrochem. Soc. **110**, 213 (1963).
[14] J. M. Sherfey and A. Brenner, J. Electrochem. Soc. **105**, 665 (1958).
[15] P. Boudeville, Inorg. Chim. Acta **226**, 69 (1994).
[16] T. Ozeki, N. Ogawa, K. Aikawa, I. Watanabe, and S. Ikeda, J. Electroanal. Chem. **145**, 53 (1983).
[17] T. Ozeki, I. Watanabe, and S. Ikeda, J. Electroanal. Chem. **96**, 117 (1979).
[18] S. Shibata and M. P. Sumino, J. Electroanal. Chem. **193**, 135 (1985).
[19] B. Hai and D. Scherson, J. Phys. Chem. C **113**, 18244 (2009).
[20] R. Schuster, R. Rösch, and A. E. Timm, Z. Phys. Chem. **221**, 1479 (2007).
[21] C. E. Borroni-Bird and D. A. King, Rev. Sci. Instrum. **62**, 2177 (1991).
[22] W. Lew, O. Lytken, J. A. Farmer, M. C. Crowse, and C. T. Campbell, Rev. Sci. Instrum. **81**, 024102 (2010).
[23] J. T. Stuckless, N. A. Frei, and C. T. Campbell, Rev. Sci. Instrum. **69**, 2427 (1998).
[24] I. Tasaki and K. Iwasa, Biochem. Biophys. Res. Commun. **101**, 172 (1981).
[25] Z. Jiang, Y. Xiang, and J. Wang, J. Electroanal. Chem. **316**, 199 (1991).
[26] H. Tautz, *Wärmeleitung und Temperaturausgleich* (Verlag Chemie, Weinheim, 1971).
[27] *CRC Handbook of Chemistry and Physics*, 85th ed., edited by D. L. Lide (CRC, New York, 2004).
[28] P. Boudeville and A. Tallec, Thermochim. Acta **126**, 221 (1988).
[29] H.-X. Wang, D. Wang, B. Li, and S. Sun, J. Electroanal. Chem. **392**, 21 (1995).
[30] H. Gerischer, Z. Elektrochemie **62**, 256 (1958).
[31] W. Mehl and J. O. M. Bockris, J. Chem. Phys. **27**, 818 (1957).
[32] P. Prod'homme, F. Maroun, R. Cortes, and P. Allongue, Appl. Phys. Lett. **93**, 171901 (2008).
[33] G. Kästle, H.-G. Boyen, B. Koslowski, A. Plettl, F. Weigl, and P. Ziemann, Surf. Sci. **498**, 168 (2002).